Supplement of Atmos. Chem. Phys., 23, 7225–7239, 2023
https://doi.org/10.5194/acp-23-7225-2023-supplement

Atmospheric Chemistry and Physics
Open Access

Supplement of

Vertical distribution of black carbon and its mixing state in the urban boundary layer in summer

Hang Liu et al.

Correspondence to: Xiaole Pan (panxiaole@mail.iap.ac.cn)

Table S1 Timetable of the vertical profile measurement

Date	Ascending start time	Ascending start time	Descending start time	Descending end time
6/15	14:01	14:25	15:01	15:31
6/17	7:04	7:34	8:15	8:45
6/17	18:03:16	18:33:39	19:15:33	19:45:47
6/17	22:00	22:30:30	23:00:05	23:30:25
6/18	7:00	7:31	8:15	8:45:25
6/18	11:00	11:30:38	12:16:20	12:46:40
6/18	18:00	18:30:30	19:15:02	19:45:20
6/24	18:00:15	18:30:40	19:15:07	19:45:22
6/24	22:00:05	22:30	23:15	23:45
6/25	7:00	7:30:30	8:15	8:45:22
6/25	11:00	11:30:37	12:15:15	12:46
6/25	18:00	18:30:22	19:15	19:45:25
6/27	18:30:15	19:00:45	19:45	20:15:20
6/27	22:00:50	22:31:15	23:14:40	23:45:30
6/28	11:00	11:30:30	12:15:09	12:45:22
6/28	18:00:01	18:30:23	19:15:04	19:45:28
6/29	11:00:03	11:30:30	12:15:03	12:45:20
6/29	18:00:05	18:30:25	19:15:05	19:45:20
6/29	22:06:10	22:36:40	23:21	23:51
6/30	7:00:05	7:30:25	8:15:05	8:45:30
6/30	10:59:55	11:30:30	12:15	12:45:16
6/30	18:00	18:30:20	19:15	19:45:40
7/1	11:00	11:30:24	12:15	12:45:12
7/1	18:00	18:30:23	19:50	20:15:00
7/1	22:00	22:30:28	23:15	23:45:22
7/2	7:00	7:30:32	8:15:04	8:45:30
7/2	11:00	11:30:30	12:15:04	12:45:30
7/2	18:00	18:30:32	19:15	19:45:25
7/2	22:00	22:30:30	23:15	12:45:30
7/7	7:04	7:34:40	8:18:11	8:48:50
7/7	11:02:16	11:32:45	12:17:06	12:47:30
7/7	18:00	18:30:30	19:15	19:45:20
7/7	22:00	22:30:40	23:15	23:45:30
7/8	7:00:29	7:30:48	8:15:05	8:45:32
7/8	11:00:11	11:30:41	12:15:10	12:45:40
7/8	18:00:00	18:30:25	19:15:10	19:45:25
7/8	22:00:00	22:30:23	23:15:05	23:45:25
7/9	11:00:00	11:30:30	12:15:00	12:45:25
7/9	18:00:02	18:30:32	19:15	19:45:30
7/9	22:00:03	22:30:35	22:46:00	23:16:35
7/10	11:00	11:30:28	12:15	12:45:25
7/10	18:00	18:30:26	19:15	19:45:30
7/10	22:00	22:30:26	23:15	23:45:20
7/11	6:00:00	06:30:25	07:15:02	7:45
7/11	11:00:00	11:30:26	12:15:05	12:45:30
7/11	18:00:00	18:30:23	19:15:06	19:42:00
7/12	22:00:00	22:30	23:15	23:45
7/13	6:00:02	6:30:30	7:15:02	7:45:30
7/13	11:00:02	11:30:30	12:15:02	12:45:30
7/13	22:00:02	22:30:30	23:15:10	23:45:42
7/14	8:00	8:30:30	9:15	9:45:30
7/14	11:00	11:30:30	12:15:05	12:45:24
7/14	22:00	22:30:33	23:15:00	23:45:20
7/15	6:00	6:30:25	7:15	7:45:46

7/15	11:03:40	11:34:00	12:15:00	12:45:20
7/15	22:00:05	22:30:25	23:15:00	23:45:20

Table S2 Brief summarize of vertical measurement about BC and its mixing state

Measurement area	Measurement description	BC conc.	BC core Size distribution	Coating thickness	Reference
Europe	Aircraft measurement (0-1000m), EUCAARI campaign.	~6-200 ng/m^3, decreasing with altitude.	With MMD of 150-210 nm, decreasing with altitude.	-	(Ding et al., 2019)
Rural Beijing	Aircraft measurement (0- 3000m).	~50-3000 ng/m^3, decreasing with altitude.	With MMD of 160-230 nm, the vertical profile of MMD varied from cases.	Higher coating thickness in the boundary layer under pollution conditions.	(Ding et al., 2019;Zhao et al., 2020)
Arctic	Aircraft measurement (0.1-5500m), NETCARE campaign	1.4-50 ng/m^3, generally decreasing with altitude, but existing concentration peaks at certain height	With MMD of 130-200 nm, decreasing with altitude in Spring but uniform in summer.	-	(Schulz et al., 2019)
Europe to North America	Aircraft measurement 2-20km)	1-40 ng/m^3, decreasing with altitude	-	Significant coating thickness increase during plume affected period	(Ditas et al., 2018)
Global	Aircraft measurement, HIPPO and Atom campaign	1-10 ng rBC/kg air in the upper troposphere, 0.5-2 ng rBC/kg in the lower stratosphere	-	-	(Katich et al., 2018;Schwarz et al., 2013;Schwarz et al., 2017)

Table S3 Brief summarize of the instruments in the moveable container

Instruments	Abbreviation	Manufactory	Measuring parameters	Resolution	Data process
Single particle soot photometer	SP2	Droplet measurement technologies	BC concentration MMD D_p/D_c	Single particle	Calculating the average properties of all observed particles in a certain time window (1 min or 1 h)
Photoacoustic extinctiometer	PAX	Droplet measurement technologies	$PM_{2.5}$ b_{sca} (λ= 870 nm)	1 second	Averaged (Arithmetic mean in 1 min) to 1 min
Aethalometer	AE33	Magee Scientific Corp.	b_{abs} (λ= 880 nm)	1 second	Averaged (Arithmetic mean in 1 min) to 1 min
49i O_3 analyzer		Thermo Scientific	O_3 concentration	1 second	Averaged (Arithmetic mean in 1 min) to 1 min
42i NO-NO_2-NO_x analyze		Thermo Scientific	NO and NO_2 concentration	1 second	Averaged (Arithmetic mean in 1 min) to 1 min
48i CO analyzer		Thermo Scientific	CO concentration	1 second	Averaged (Arithmetic mean in 1 min) to 1 min

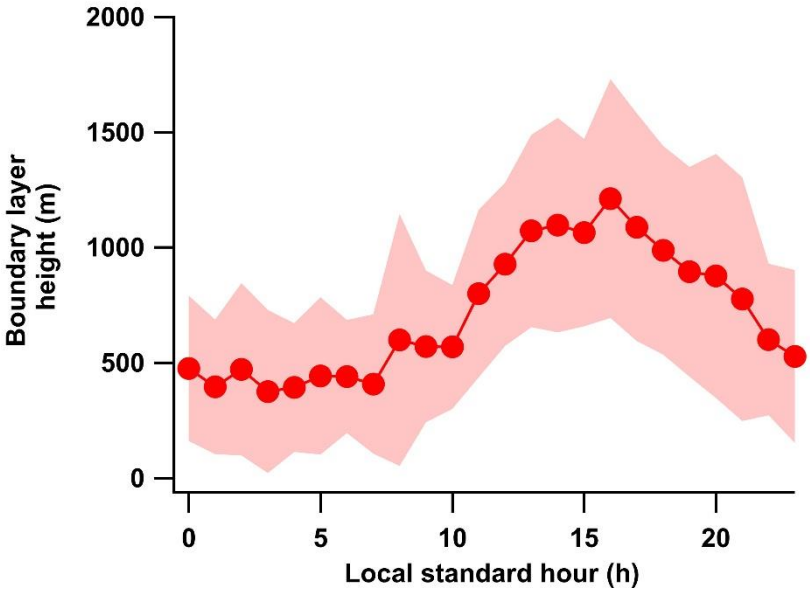

Figure. S1 Diurnal variation of BLH during the observation.

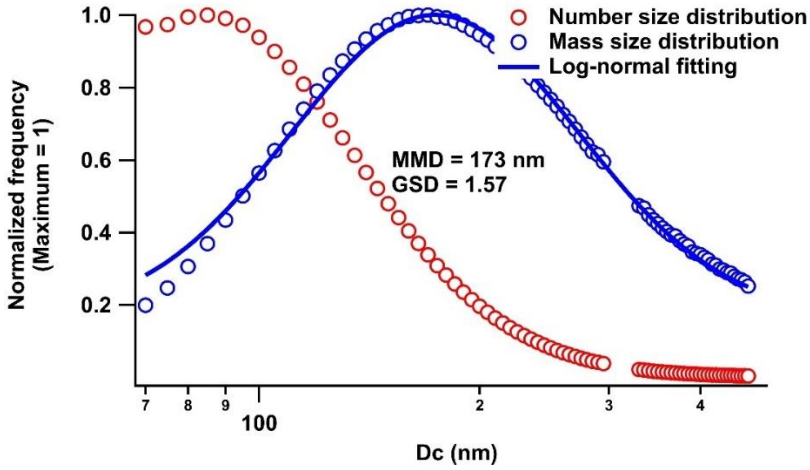

Figure. S2 Size distribution of BC core during the entire observation.

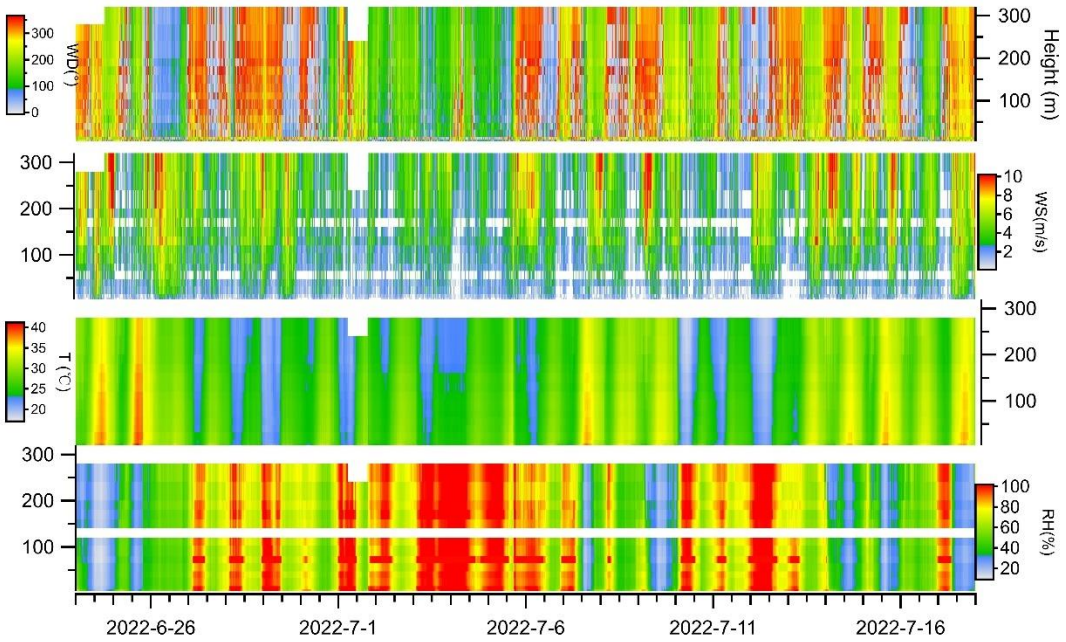

Figure. S3 Meteorology conditions (0-320 m) during the observation period.

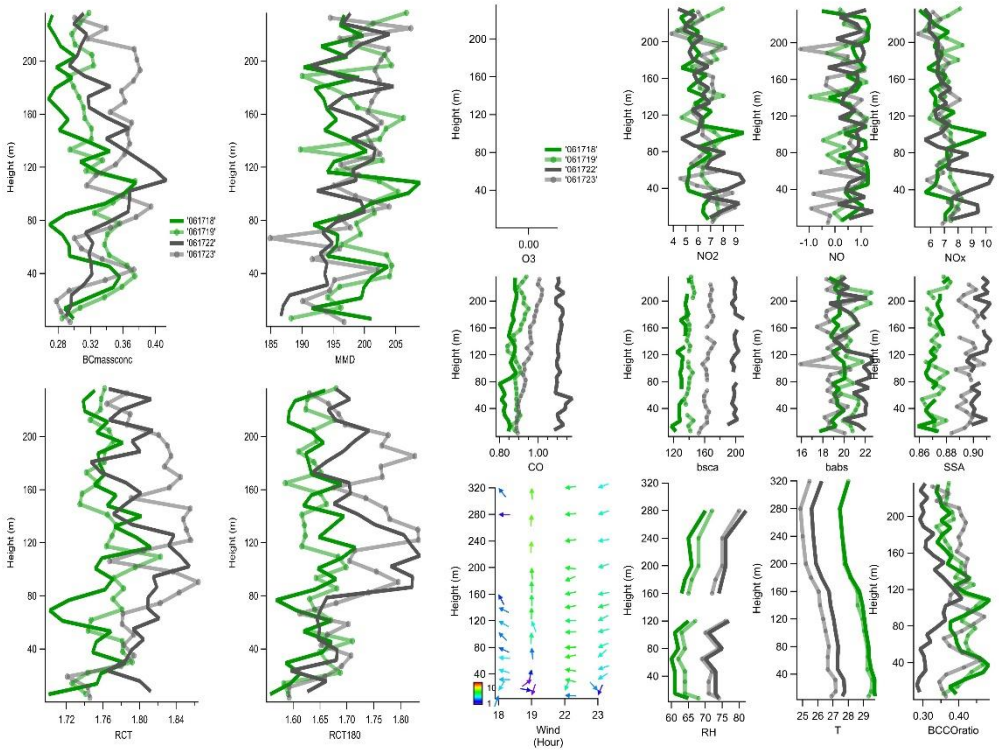

Figure S4 Vertical profiles during 17th June. RCT denotes D_p/D_c and RCT180 denotes the D_p/D_c for BC with D_c = 180±10 nm.

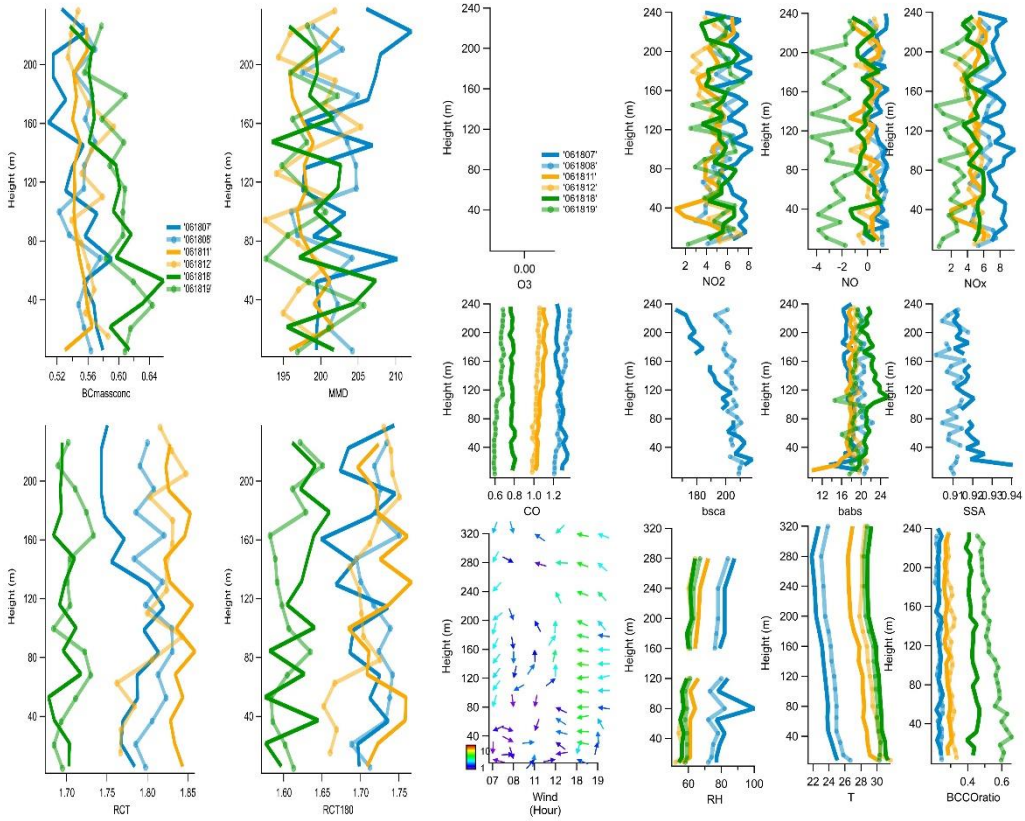

Figure S5 Vertical profiles during 18th June

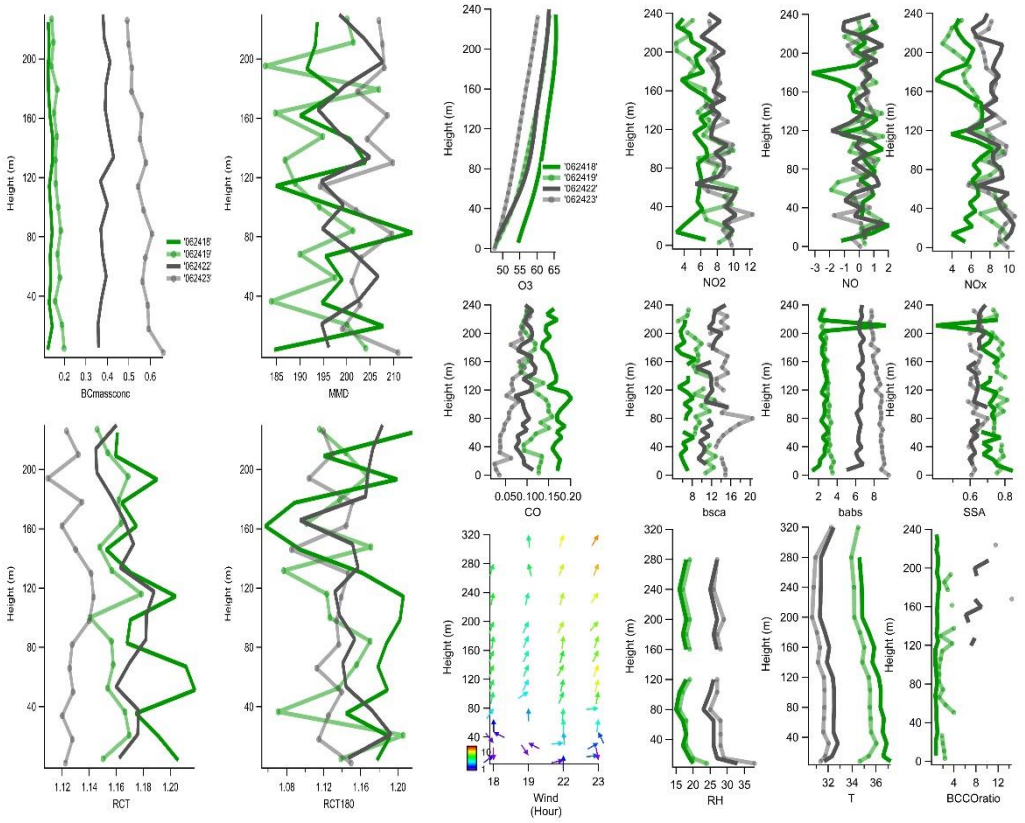

Figure S6 Vertical profiles during 24th June

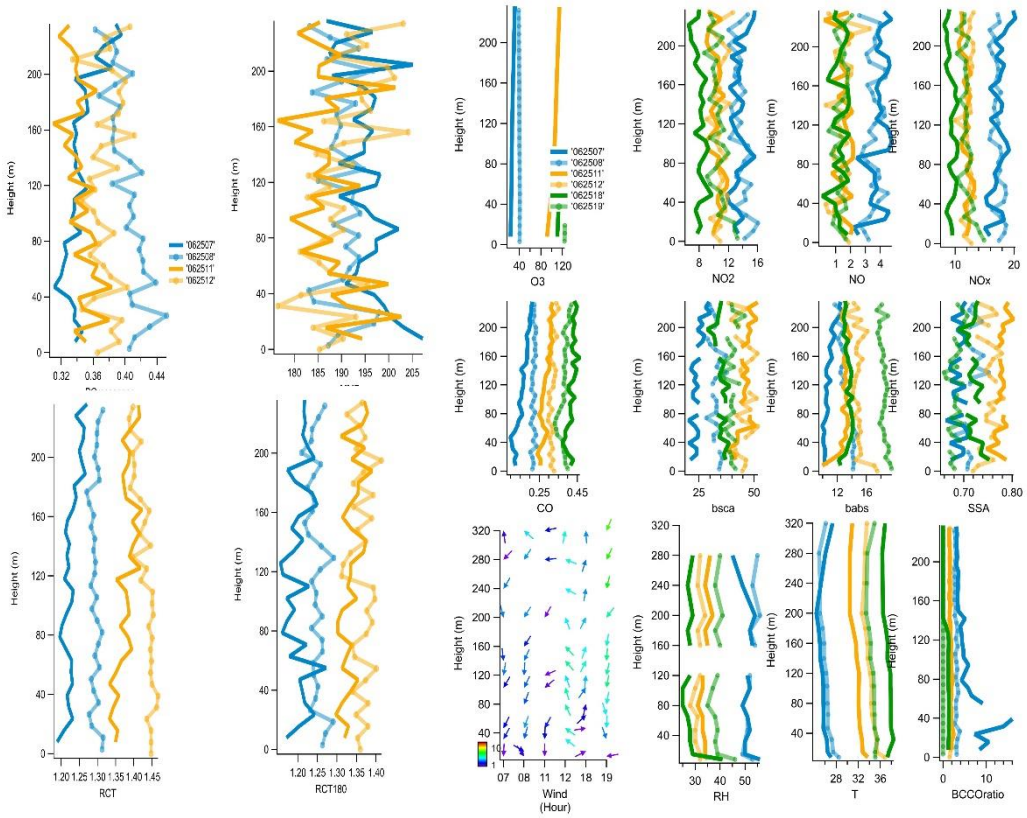

Figure S7 Vertical profiles during 25th June

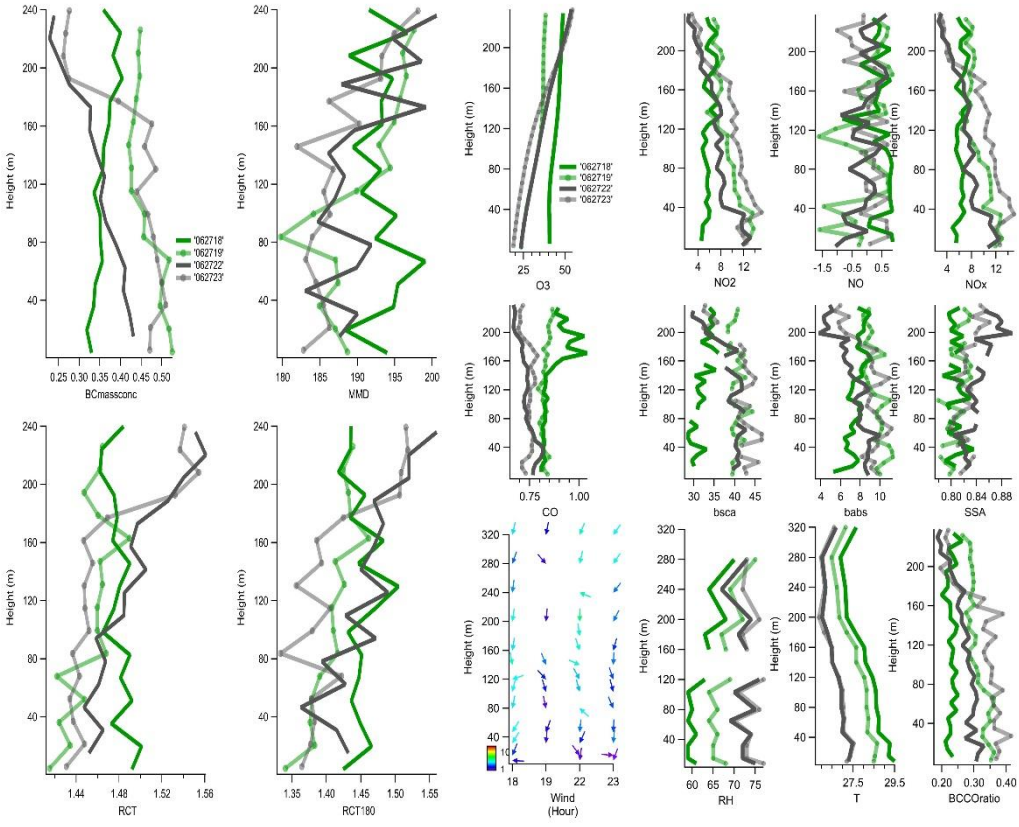

Figure S8 Vertical profiles during 27th June

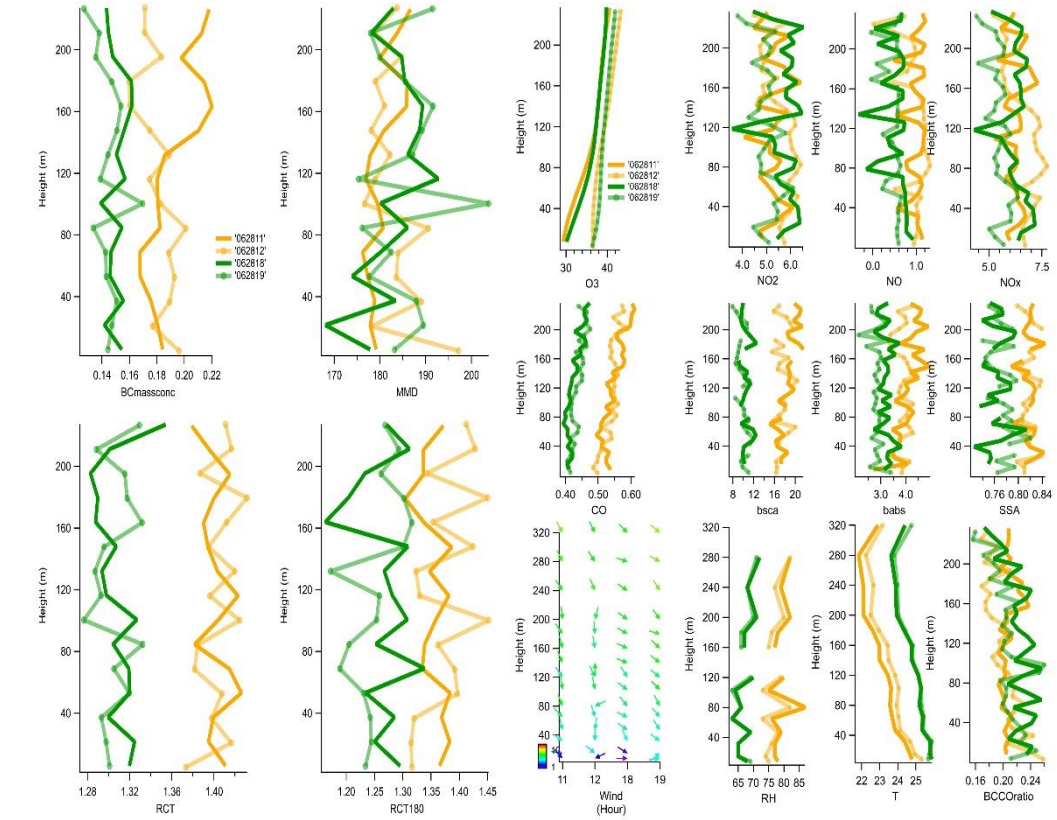

Figure S9 Vertical profiles during 28th June

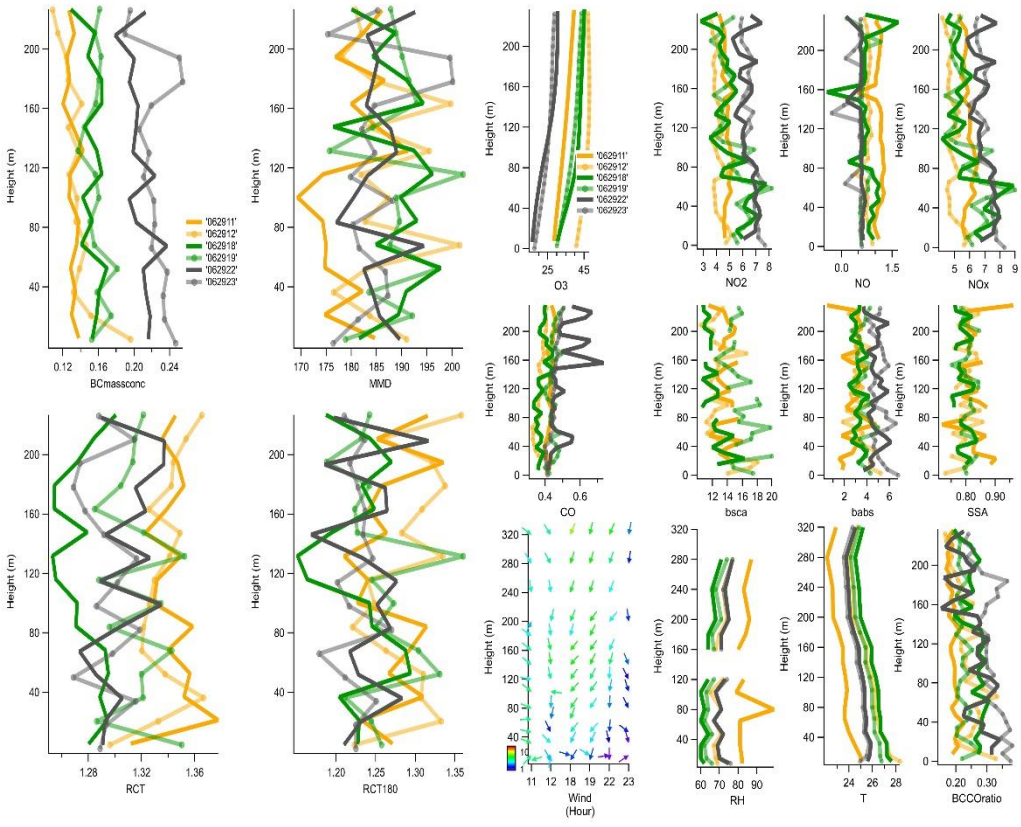

Figure S10 Vertical profiles during 29th June

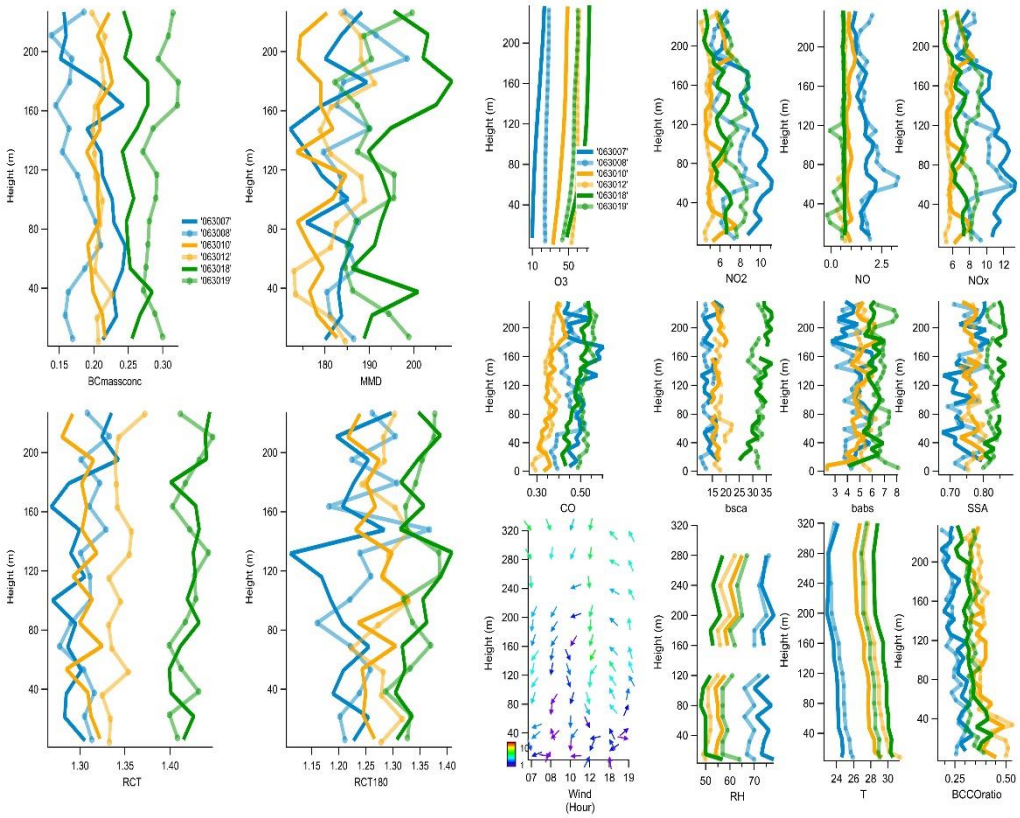

Figure S11 Vertical profiles during 30th June

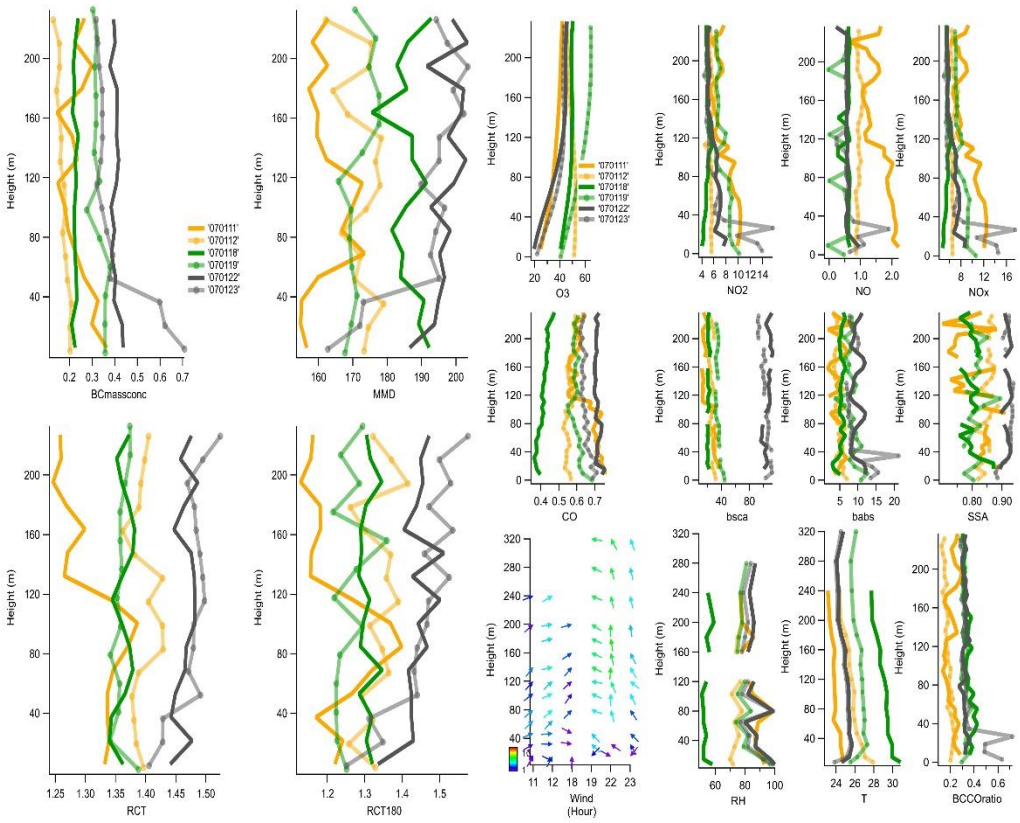

Figure S12 Vertical profiles during 1st July

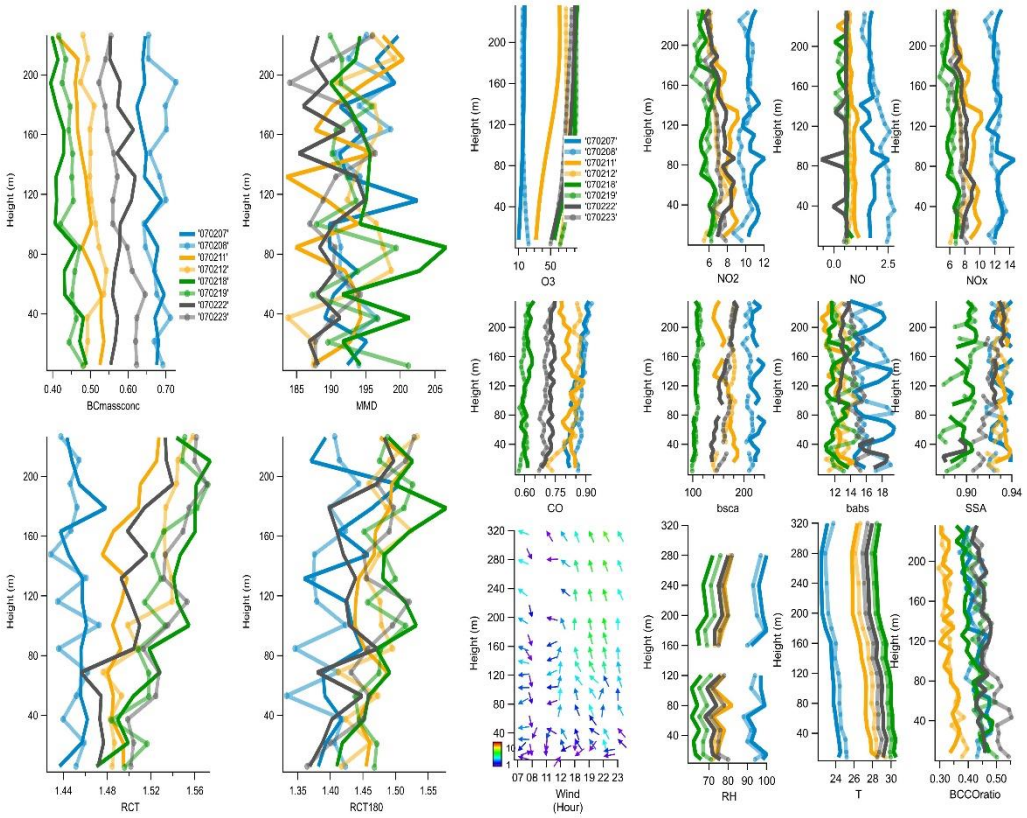

Figure S13 Vertical profiles during 2nd July

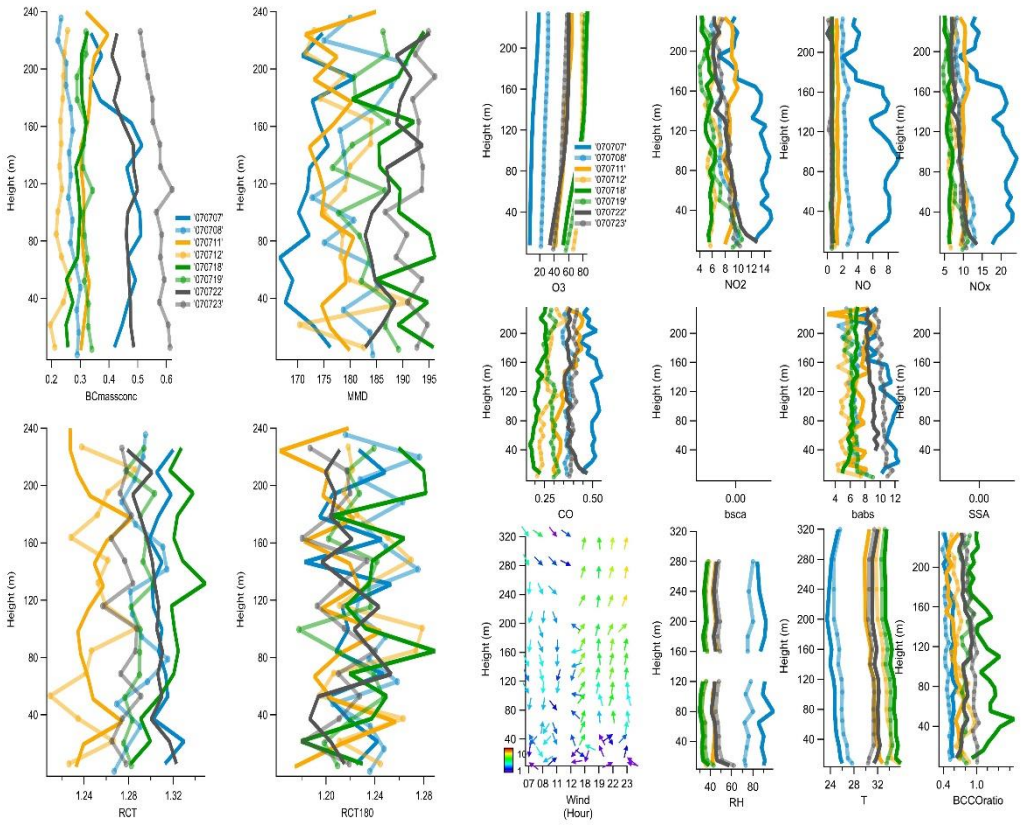

Figure S14 Vertical profiles during 3rd July

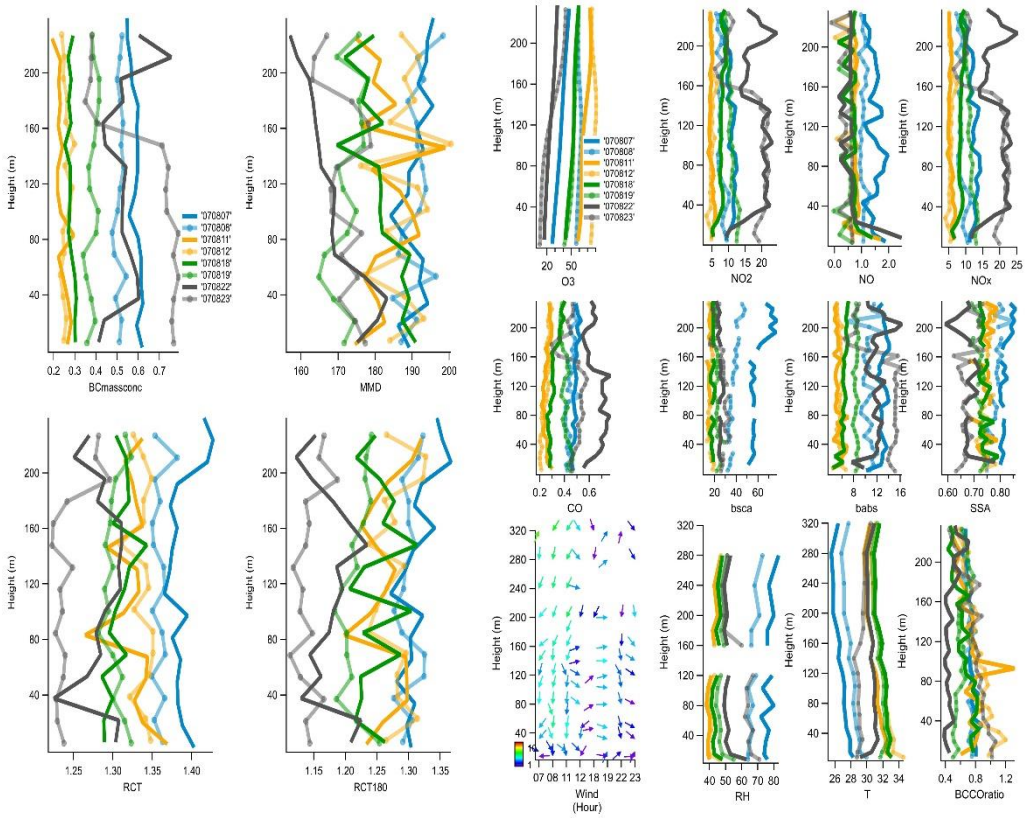

Figure S15 Vertical profiles during 8th July

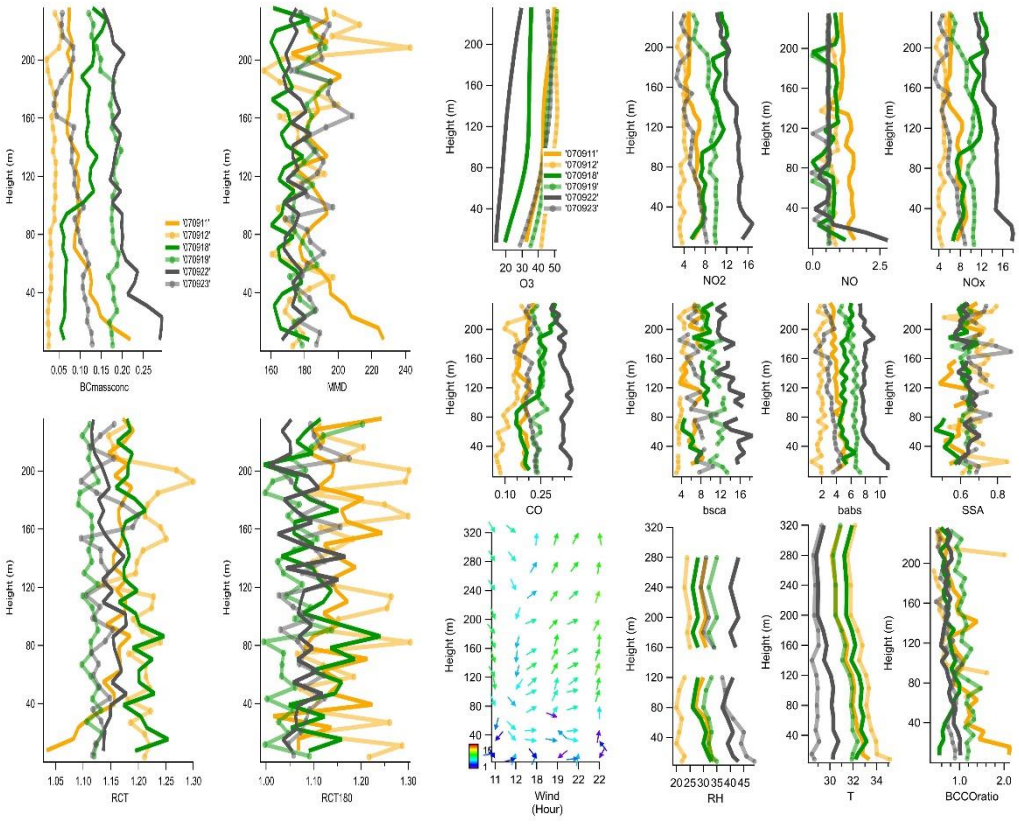

Figure S16 Vertical profiles during 9th July

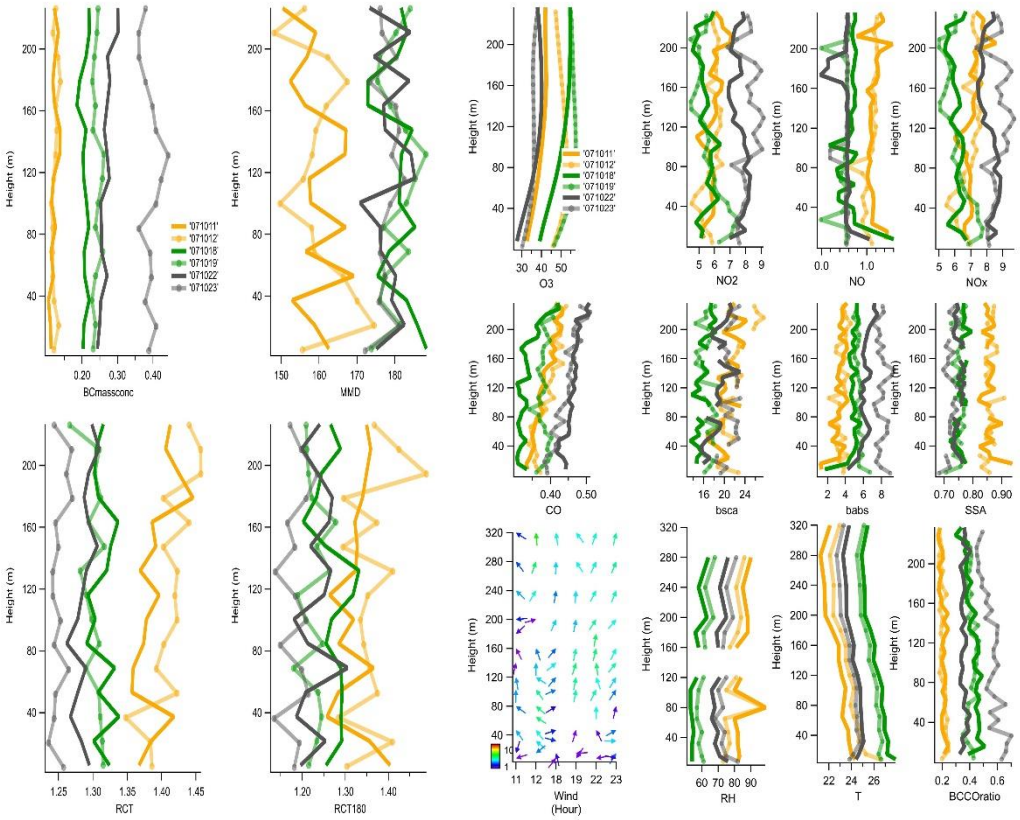

Figure S17 Vertical profiles during 10th July

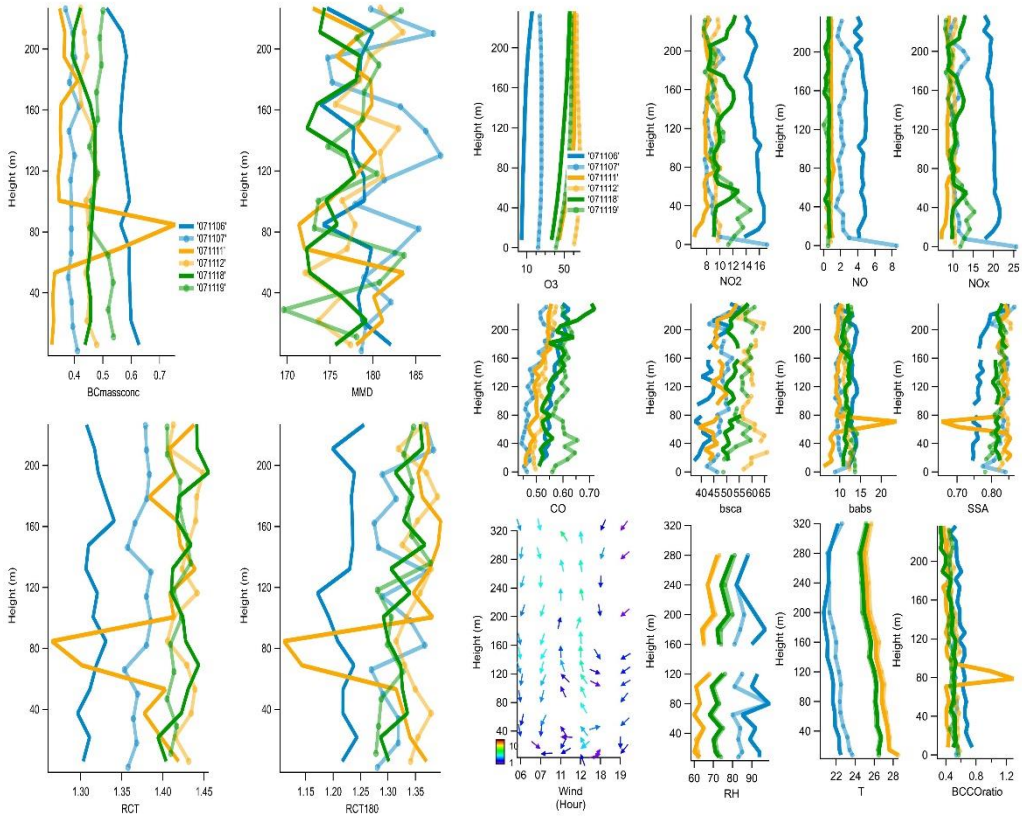

Figure S18 Vertical profiles during 11th July

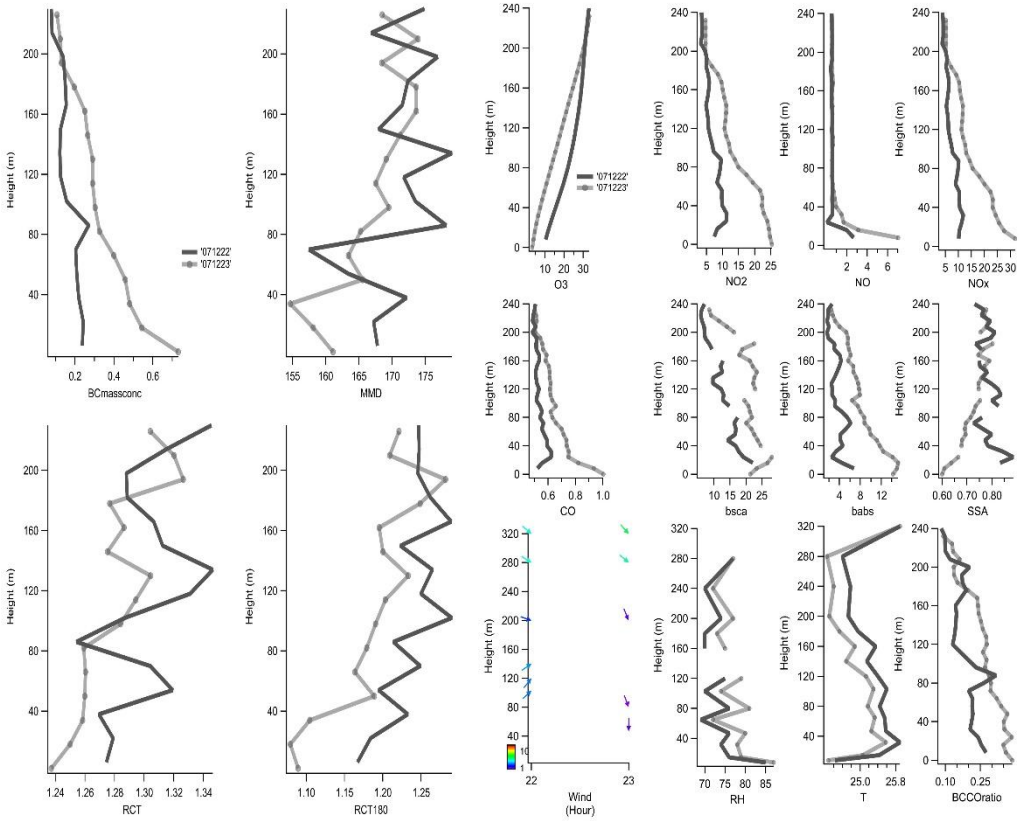

Figure S19 Vertical profiles during 12th July

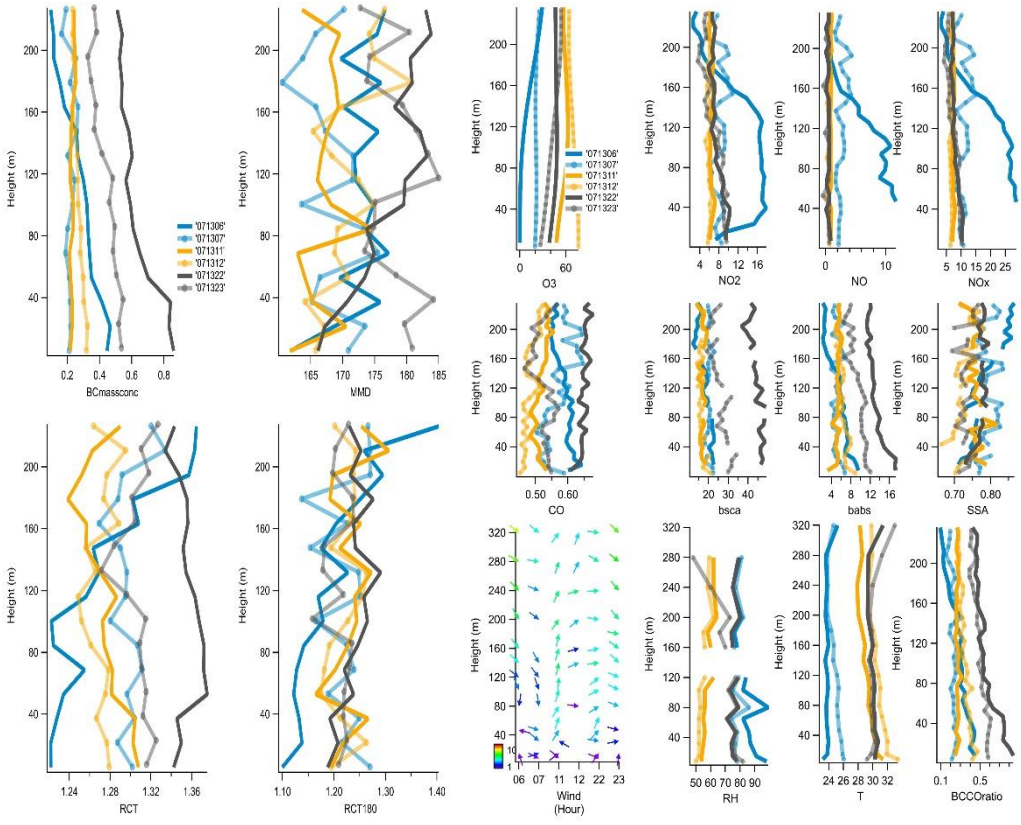

Figure S20 Vertical profiles during 13th July

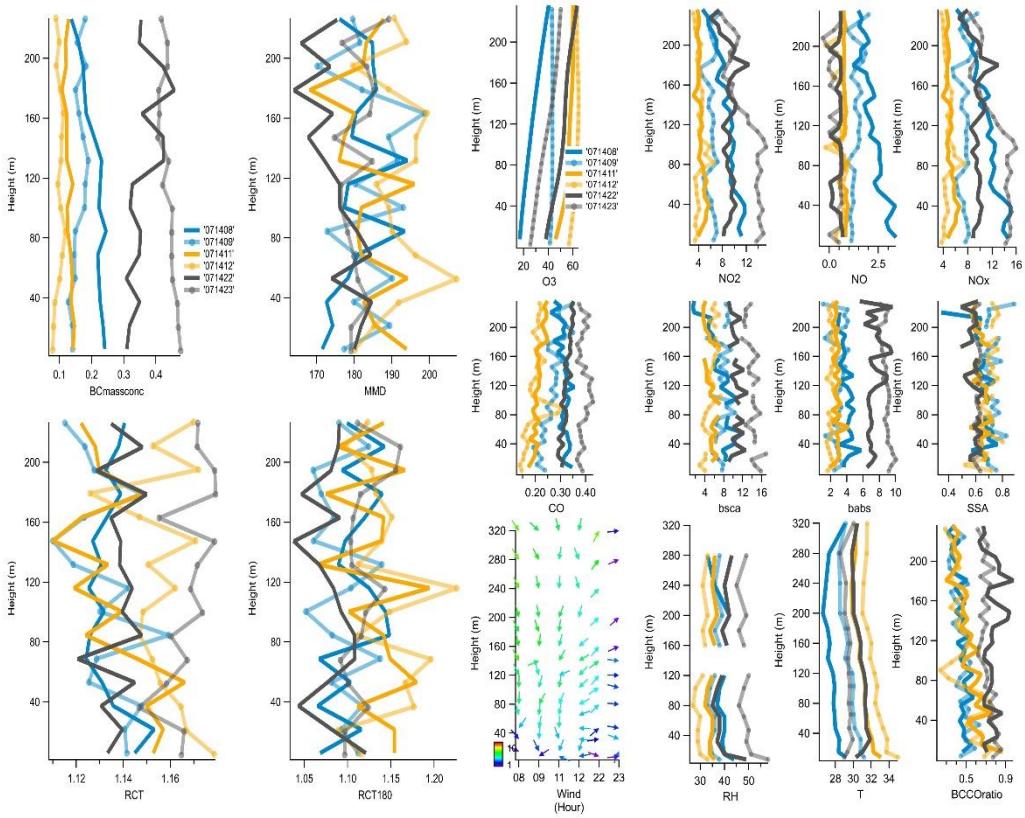

Figure S21 Vertical profiles during 14th July

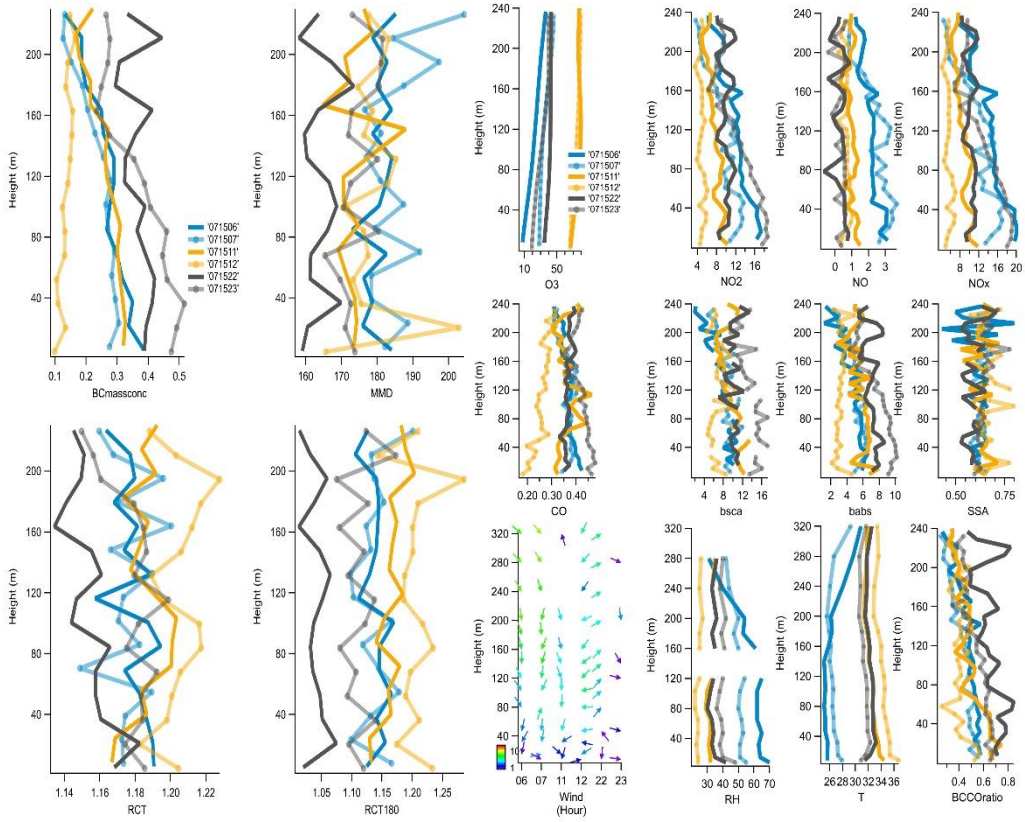

Figure S22 Vertical profiles during 15th July

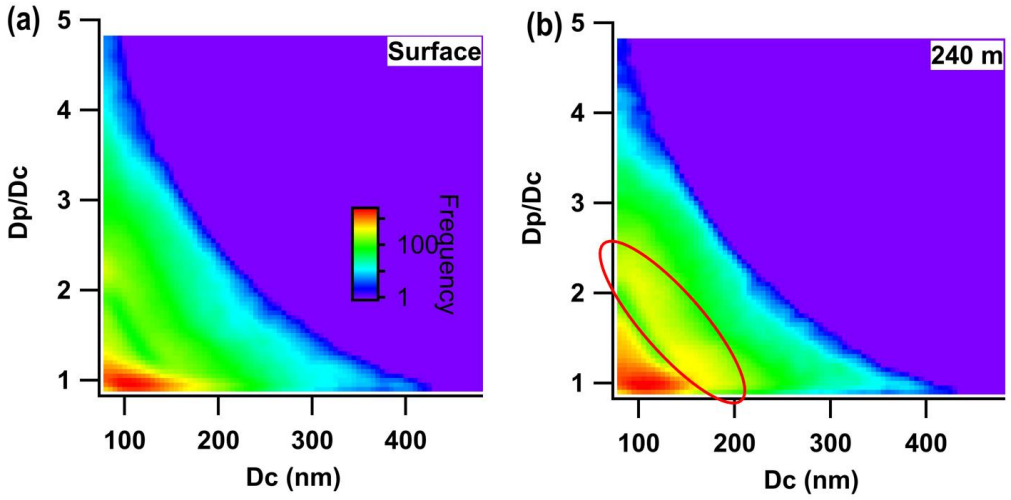

Figure S23 The size-resolved D_p/D_c at 23:00 27th June. (a) the surface level, (b) the 240 m level.

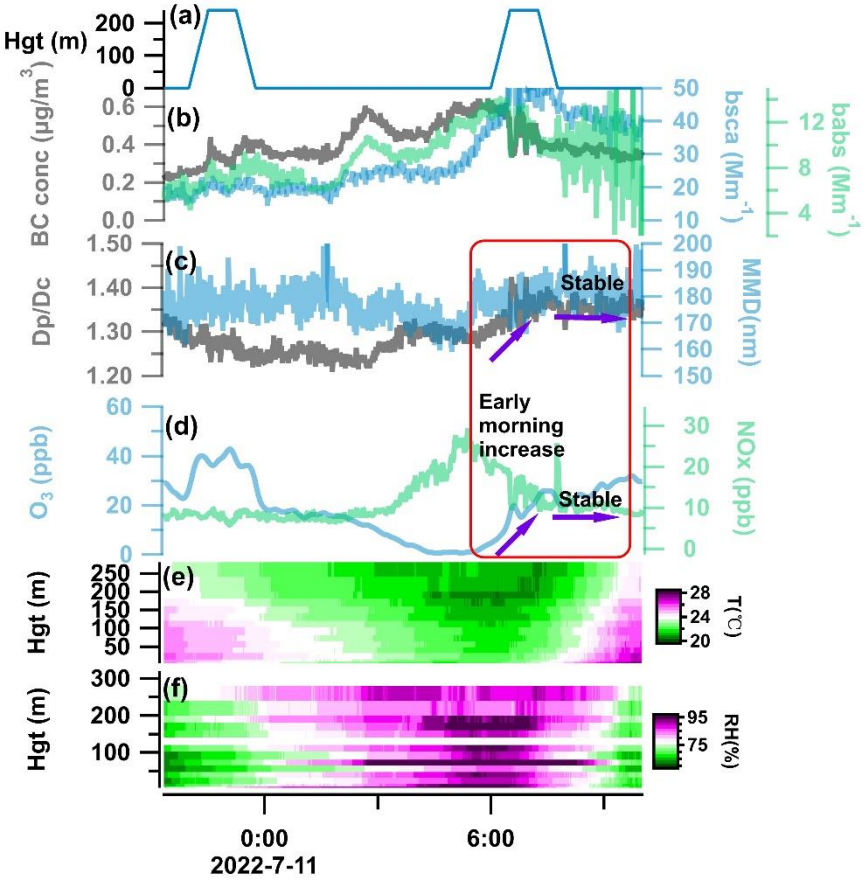

Figure S24 Another case of vertical mixing leading to the increase of O_3 and D_p/D_c in the morning.

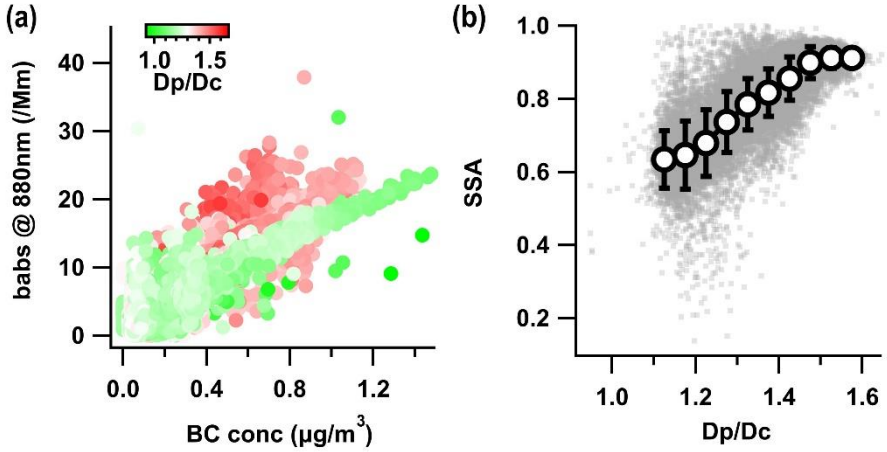

Figure S25 (a)The relationship between BC concentration and b_{abs}. (b)The relationship between SSA and D_p/D_c.

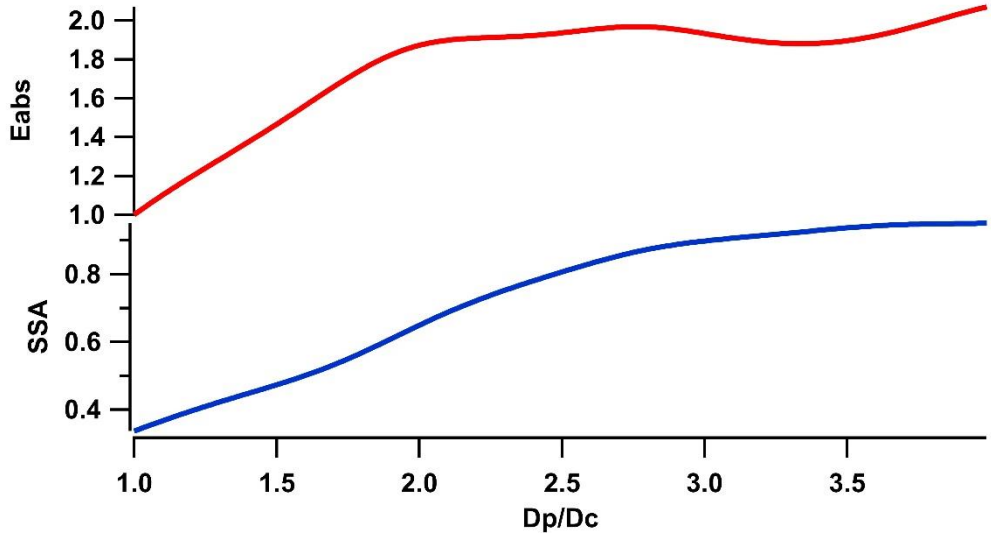

Figure S26 The variation of E_{abs} and SSA with D_p/D_c for BC-containing particles with D_c=170 nm through Mie-theory.

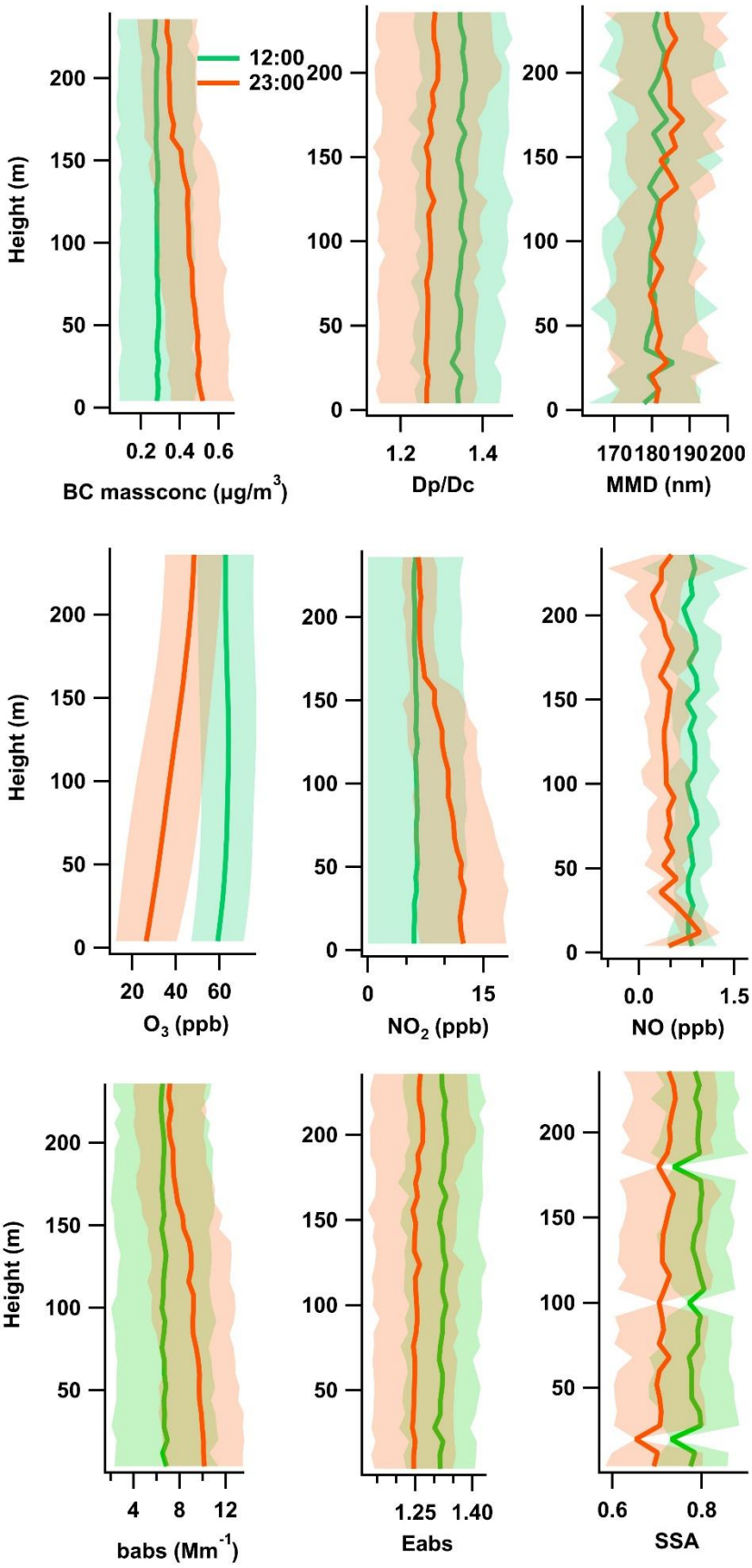

Figure S27 The same as Fig. 4 but with error bars.

References

Ding, S., Liu, D. T., Zhao, D. L., Hu, K., Tian, P., Zhou, W., Huang, M. Y., Yang, Y., Wang, F., Sheng, J. J., Liu, Q., Kong, S. F., Cui, P. Y., Huang, Y. D., He, H., Coe, H., and Ding, D. P.: Size-Related Physical Properties of Black Carbon in the Lower Atmosphere over Beijing and Europe, Environ Sci Technol, 53, 11112-11121, 10.1021/acs.est.9b03722, 2019.

Ditas, J., Ma, N., Zhang, Y., Assmann, D., Neumaier, M., Riede, H., Karu, E., Williams, J., Scharffe, D., Wang, Q. Q., Saturno, J., Schwarz, J. P., Katich, J. M., McMeeking, G. R., Zahn, A., Hermann, M., Brenninkmeijer, C. A. M., Andreae, M. O., Poschl, U., Su, H., and Cheng, Y. F.: Strong impact of wildfires on the abundance and aging of black carbon in the lowermost stratosphere, P Natl Acad Sci USA, 115, E11595-E11603, 10.1073/pnas.1806868115, 2018.

Katich, J. M., Samset, B. H., Bui, T. P., Dollner, M., Froyd, K. D., Campuzano-Jost, P., Nault, B. A., Schroder, J. C., Weinzierl, B., and Schwarz, J. P.: Strong Contrast in Remote Black Carbon Aerosol Loadings Between the Atlantic and Pacific Basins, J. Geophys. Res.-Atmos., 123, 13386-13395, 10.1029/2018jd029206, 2018.

Schulz, H., Zanatta, M., Bozem, H., Leaitch, W. R., Herber, A. B., Burkart, J., Willis, M. D., Kunkel, D., Hoor, P. M., Abbatt, J. P. D., and Gerdes, R.: High Arctic aircraft measurements characterising black carbon vertical variability in spring and summer, Atmospheric Chemistry and Physics, 19, 2361-2384, 10.5194/acp-19-2361-2019, 2019.

Schwarz, J. P., Samset, B. H., Perring, A. E., Spackman, J. R., Gao, R. S., Stier, P., Schulz, M., Moore, F. L., Ray, E. A., and Fahey, D. W.: Global-scale seasonally resolved black carbon vertical profiles over the Pacific, Geophysical Research Letters, 40, 5542-5547, 10.1002/2013gl057775, 2013.

Schwarz, J. P., Weinzierl, B., Samset, B. H., Dollner, M., Heimerl, K., Markovic, M. Z., Perring, A. E., and Ziemba, L.: Aircraft measurements of black carbon vertical profiles show upper tropospheric variability and stability, Geophysical Research Letters, 44, 1132-1140, 10.1002/2016gl071241, 2017.

Zhao, D. L., Liu, D. T., Yu, C. J., Tian, P., Hu, D. W., Zhou, W., Ding, S., Hu, K., Sun, Z. B., Huang, M. Y., Huang, Y., Yang, Y., Wang, F., Sheng, J. J., Liu, Q., Kong, S. F., Li, X. M., He, H., and Ding, D. P.: Vertical evolution of black carbon characteristics and heating rate during a haze event in Beijing winter, Sci Total Environ, 709, ARTN 136251
10.1016/j.scitotenv.2019.136251, 2020.